

# Vertical Polarized Antennas for Low-VHF Radio Meteor Detection

Cezar-Eduard Lesanu<sup>1</sup>, Adrian Done<sup>2</sup>, Alin-Mihai Căilean<sup>1,2</sup>, Adrian Graur<sup>1,2</sup>

<sup>1</sup>Department of Computers, Electronics and Automation, Stefan cel Mare University of Suceava, 13 Universitatii, 720229, Suceava, Romania

<sup>2</sup>Integrated Center for research, development and innovation in Advanced Materials, Nanotechnologies, and Distributed Systems for fabrication and control, Stefan cel Mare University of Suceava, Suceava, Romania

**Abstract—** The study of meteors by radio using a bistatic RADAR configuration in the Low-VHF portion of the spectrum requires the use of receiving antennas that are not always easy to install while fulfilling the imposed requirements. In order to facilitate the implementation of radio meteor detection stations that operate in this frequency range, the parameters of vertical antennas with unusual characteristics were analyzed. These antennas are characterized as having uncommon features in term of geometry and radiation patterns, whereas they should be simple to build, feed and install. Based on this analysis, a directive vertical antenna array which exhibits by design the features that make it suitable for radio meteor detection is proposed and preliminary results are provided.

**Keywords—** *bistatic radar; directive antennas; radio meteor detection; vertical polarized antennas.*

## I. INTRODUCTION

The detection of meteors by radio is a branch of radio astronomy that studies the distribution of the meteoroids in our region of the Solar System. The meteoroids are the smallest celestial bodies, particle of dust and lumps of rock or iron that orbit the Sun and they are characterized as having a dimension of up to one meter [1], [2]. At the entrance into the atmosphere, the meteoroids disintegrate due to their very high speed (i.e. ~40 km/s in average) and create a channel of plasma that is called meteor, the visible phenomenon a.k.a. “falling star”. The atmospheric region of occurrence of meteor plasma trails spreads between 80 km and 120 km in altitude.

Generally, the meteoroids are too small to be detected by RADAR techniques. On the other hand, the meteor trails are large enough, whereas the plasma from which they are made (i.e. the free electrons) has the property of reflecting the radio waves. The frequency range in which the reflections occur has the lower limit imposed by the presence of the ionosphere (i.e. at about 30 MHz) and the upper imposed by the physical proprieties of the plasma [3]. Due to these properties, as the frequency increases the number of reflections decreases.

One type of meteor radio detection system is the bistatic

---

The infrastructure used in this work was supported from the project “Integrated Center for research, development and innovation in Advanced Materials, Nanotechnologies, and Distributed Systems for fabrication and control”, Contract No. 671/09.04.2015, Sectoral Operational Program for Increase of the Economic Competitiveness co-funded from the European Regional Development Fund.

RADAR that makes use of dedicated radio beacons or opportunity transmitters as sky illuminators [4]. In a bistatic RADAR, the transmitter and the receiver are situated reciprocally below the radio horizon, so that there is no direct radio visibility between the two (see Fig. 1). When a meteor appears in the coverage area, the radio waves are reflected by the meteor trail and then they reach the receiver. The baseline (i.e. ground distance between the transmitter and receiver) ranges from about 150 km and up to 2000 km. At lower ranges, the direct radio waves interfere with the meteor reflections, whereas at higher ranges the curvature of the Earth prevents these reflections to take place. Geographic topographies like mountains can reduce the usable baseline of a bistatic RADAR.

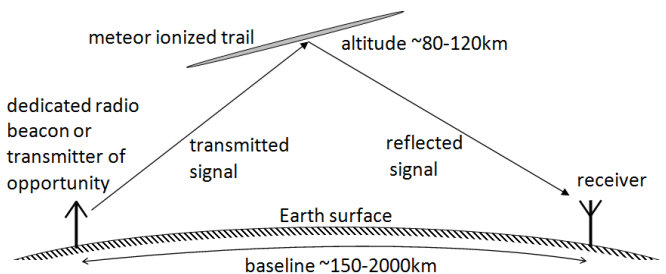


Fig. 1. Bistatic RADAR configuration for radio meteor detection

Unlike the dedicated radio meteor beacons which have known polarization (i.e. usually circular), opportunity transmitters have various polarizations (i.e. vertical, horizontal or circular), which in some cases are unknown. The polarization of the receiving antennas for bistatic radio meteor detection used in existing active networks may be simple linearly polarized, (i.e. vertical or horizontal) or it can have twin or circular polarization in the more elaborated systems [5], - [9]. Worth mentioning that the geometry of reflection on meteor trails and the Faraday Effect change the polarization of radio waves on the path from transmitter to receiver. As a result, the radio waves that reach the receiving antenna are randomly polarized.

In the above mentioned context, this paper focuses on the usage of receiving antennas for bistatic radio meteor detection systems that operate in the Low-VHF frequency band (30 – 88

MHz). The baselines of interest, low and medium ranges comprised between 150 and 500 km, requires the use of antennas with the main lobe at 20° to 60° elevation angles above the horizon. Thus, this paper is concentrated on the design of vertically polarized antennas which exhibit by design adequate features which make them suitable for radio meteor detection.

## II. VERTICAL ANTENNAS RADIATION PATTERN OVERVIEW

According to [10], [11] vertical antennas with atypical physical lengths of the radiator (odd multiples of  $\lambda/4$ ) have high elevation angles of the main lobe, making them suitable for applications in which the space wave is desirable. Previous experiments [12], [13] have showed that a three quarter wavelength vertical ( $3\lambda/4$ ) antenna can provide reliable results in a bistatic radar system for radio meteor detection. Nevertheless, this paper addresses the issue in a more detailed manner, and it introduces a new directive vertical polarized antenna.

Fig. 2 illustrates a comparison between the radiation patterns in the vertical plane of several vertical antennas with various radiator lengths. The  $\lambda/4$ ,  $\lambda/2$  and  $5\lambda/8$  vertical antennas are well known and commonly used for terrestrial communications.

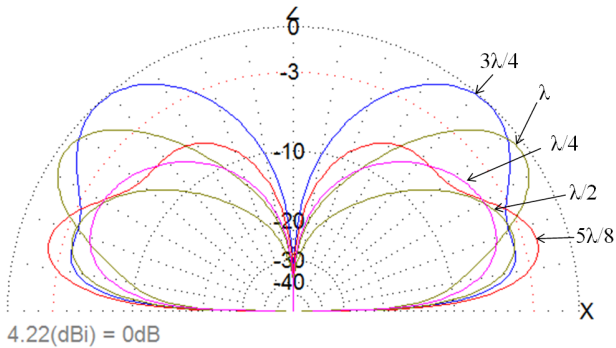


Fig. 2. Vertical antennas far field radiation pattern comparison

One can clearly see that the  $3\lambda/4$  wavelength antenna has the highest gain at medium elevation angles. The characteristics of  $3\lambda/4$  wavelength antenna can be summarized as follows:

- Favorable radiation pattern, in the vertical plane, at medium elevation angles (i.e. up to  $\sim 4$  dBi gain at 45° elevation and Half Power Beam Width (HPBW)  $\approx 40^\circ$ );
- Omnidirectional radiation pattern in the horizontal plane, obtained if symmetrically arranged radial elements are used (implementation of a MIMO-type system using multi-transmitter/multi-frequency architecture);
- End-fed, low characteristic impedance – easy to build and feed with regular coaxial transmission lines ( $50/75 \Omega$  impedance).

It can be also noticed that even at low elevation angles, the  $3\lambda/4$  wavelength vertical antenna has the gain equal or higher

than half ( $\lambda/2$ ) respectively quarter ( $\lambda/4$ ) wavelength vertical antennas.

## III. THREE QUARTER WAVELENGTH VERTICAL ANTENNA

Based on the previous observations, Fig. 3 illustrates the analysis of  $3/4$  wavelength vertical antenna fitted with one, two and four radials orthogonal to the radiator. Tuned radial elements, elevated and decoupled from the ground, are used in order to minimize the ground losses.

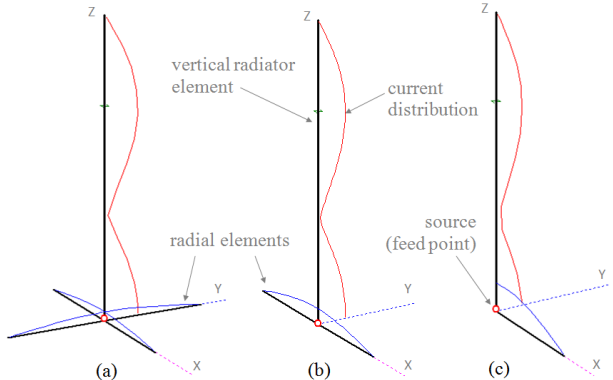
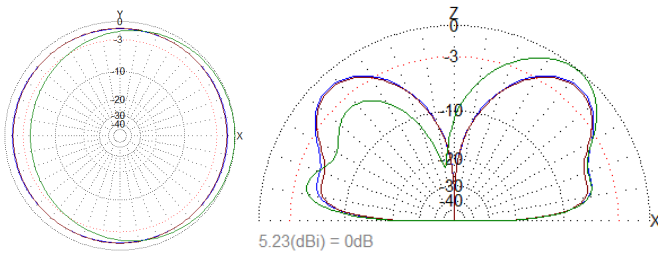


Fig. 3. Three quarter wavelength ( $3\lambda/4$ ) vertical antenna geometry and current distribution: four radials (a), two radials (b), one radial (c).

The simulations were carried out using the antenna analyzer software MMANA-GAL [14], for an antenna tuned in the Low-VHF frequency band (around 50 MHz). The chosen height was 0.1 m Above Ground Level (AGL), the elements were made of copper wire 3 mm in diameter and medium ground properties were considered (dielectric permittivity  $\epsilon = 13$  F/m, conductivity  $\sigma = 5$  mS/m).

A comparison between the radiation patterns in the horizontal and the vertical planes of a  $3/4$  wavelength vertical antenna with one, two and four radials is illustrated in Fig. 4. One can see that the usage of four radial elements provides an omnidirectional radiation pattern in the horizontal plane. In this case, the maximum gain is  $G_a \approx 4$  dBi at  $45^\circ$  elevation. The usage of only two elevated radials still keeps the omnidirectional radiation pattern within low gain margins (less than 0.2 dB @ 0.1m AGL and 1dB @ 1m AGL for 6m wavelength), as long as the two radials are placed symmetrical around the radiator. This small increase in gain (directivity) is present in the direction orthogonal to the plane defined by the antenna elements (radiator and radials). When using one radial element, the radiation pattern changes, and a higher gain is obtained in the direction of the radial. At  $50^\circ$  elevation, the maximum gain is  $G_a = 5.2$  dBi and the front to back ratio is  $F/B \approx 4$  dB.

The impedance of a three quarter wavelength vertical antenna ranges from nearly  $50 \Omega$  when the radial elements are orthogonal to the radiator, and goes up to  $100 \Omega$  when using one radial collinear with the radiator. The antenna can be matched to  $75 \Omega$  by tilting the radial ( $\sim 110^\circ$  between the radial element and the vertical radiator). The end fed design allows a lightweight structure to be used as antenna pole (e.g. fiberglass telescopic pole).



F (MHz)	R	jX	SWR	Gh	Ga	F/B	Elev.	GND	Height	Pol.
49.4	55.555	0.658	1.11	---	4.14	-0.0	46.4	Real	0.1	V
49.7	57.277	1.533	1.15	---	4.21	-0.11	46.5	Real	0.1	V
59.25	48.024	0.018	1.04	---	5.23	4.11	50.4	Real	0.1	V

Fig. 4. Three quarter wavelength ( $3\lambda/4$ ) vertical antenna theoretical far field radiation pattern comparison: four radial elements (blue), two radials (red), one radial (green).

The radiation pattern of a three quarter wavelength vertical antenna fitted with one radial element was experimentally determined by using low Earth orbit NOAA POES weather satellites as reference transmitters [15], [16]. These artificial satellites have near circular polar orbits and are stabilized in attitude. They continuously transmit an FM modulated signal with a bandwidth of 34 kHz, in the 137 MHz band, with 37 dBm of constant power [17] - [19]. The transmission VHF Real-time Antenna (VRA) onboard the satellite is a circularly polarized Quadrifilar Helix Antenna (QFH), which has an omnidirectional radiation pattern and it is always oriented orthogonal toward the Earth's surface. These features make this category of artificial satellites suitable to be used as reference radio sources for antenna pattern measurements in real environments.

A three quarter wavelength vertical antenna with one radial element, scaled for the 137 MHz band, was built and installed in a convenient place (Fig. 5 left). The Antenna Under Test (AUT) was connected to a computer controlled communication receiver ICOM PCR1000, which sends the Received Signal Strength Indicator (RSSI) signal via the COM port to a PC (Fig. 5 right). The real antenna characteristic in the vertical plane was plotted with the Signal Plotter application available in the APT-Decoder Software [20]. This software is dedicated to the weather satellite picture reception in Automatic Picture Transmission (APT) format and it ensures the receiver control and the Doppler Effect compensation. The relative path loss satellite - AUT was taken into account when plotting the real antenna characteristic. Fig. 6 presents the experimental determination (yellow) of the far field radiation pattern in the vertical plane of a three quarter wavelength vertical antenna fitted with one radial element. This experimental characteristic was traced during a pass of the NOAA 19 satellite at a maximum elevation angle of 80.8°. The theoretical radiation pattern of this antenna with the feed point at 0.1 m AGL is superimposed on this graphic as well (white). As expected, there is a higher gain at medium elevation angles in the direction of the radial element. The main lobe is split and there are other secondary lobes due to the influences of the effective height above the ground, due to the real ground properties and due to the parasitic reflections on nearby reflective structures.

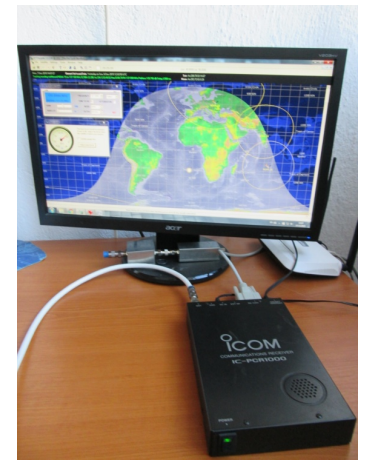


Fig. 5. Antenna radiation pattern measurement setup.

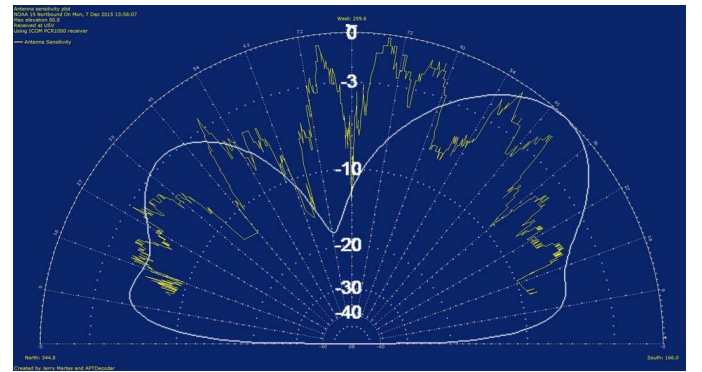


Fig. 6. Three quarter wavelength ( $3\lambda/4$ ) vertical antenna with one radial: experimental (yellow) and theoretical (white) far field radiation pattern.

A three quarter wavelength vertical antenna with one radial, optimized for  $75 \Omega$  impedance was built and integrated in the radio meteor detection sensor prototype ROAN@USV [12]. This receiving station is installed at the Astronomical Observatory and Planetarium of Stefan cel Mare University of Suceava (Romania) and it currently uses an opportunity transmitter as sky illuminator (i.e. the video carrier on 59.258MHz of an analog TV station).

#### IV. DIRECTIVE THREE QUARTER WAVELENGTH VERTICAL ANTENNA ARRAY

There are situations when a higher antenna gain is necessary at the reception in order to enhance the sensitivity of the system (link budget transmitter – meteor – receiver). Such an instance is when using low gain transmitting antennas and low emission power (low Effective Radiated Power (ERP)), as is the case of dedicated radio beacons for bistatic radio meteor detection. For this purpose, the Yagi-Uda antennas are commonly in use [5] - [8]. In their case, the increase of the elevation angle of the main radiation lobe is obtained by placing the antenna at the proper height above the ground and by tilting the antenna boom.

This paper proposes a vertical polarized antenna array with medium elevation angle of the main radiation lobe, based on the three quarter wavelength vertical radiator as an alternative

to the Yagi-Uda antennas. Similar to other directive antennas designs that employ parasitic elements, the most renown being the Yagi-Uda design, a reflector and one or more director elements are used.

In a first design of a three element vertical directive antenna, a  $3\lambda/4$  vertical radiator fitted with one radial element is used (see Table I and Fig. 7). Each one of the parasitic elements, reflector and director, has L-shape and it is composed by two segments, one vertical element about  $3\lambda/4$  in length and a  $\lambda/4$  horizontal element (radial).

The simulations performed with the antenna analyzer software MMANA-GAL show the feasibility of the design. As it was expected, a higher gain at medium elevation angle of the main lobe is obtained. These features of the radiation pattern are obtained with the antenna placed at 0.1 m AGL. After optimization, the following relative dimensions of the elements and the distances between them were obtained at the resonant frequency ( $\lambda = 5.97$  m) (see Fig. 7). The results of these simulations are illustrated in Fig. 8 – 11 and summarized in TABLE II. Fig. 8 illustrates the radiation pattern in the vertical and the horizontal planes for the  $3\lambda/4$  directive antenna with one radial. One can see that the maximum gain of this antenna is 8.8 dBi at  $44^\circ$  elevation. Fig. 9 and 10 illustrate the simulated electrical parameters of the antenna. At resonance, the reactive component of the impedance is close to zero, and the total impedance of the antenna is about  $50 \Omega$  (Fig. 9). The SWR is close to 1:1 at the same resonant frequency, whereas the bandwidth for an SWR < 1.5 is 856 kHz (Fig. 10).

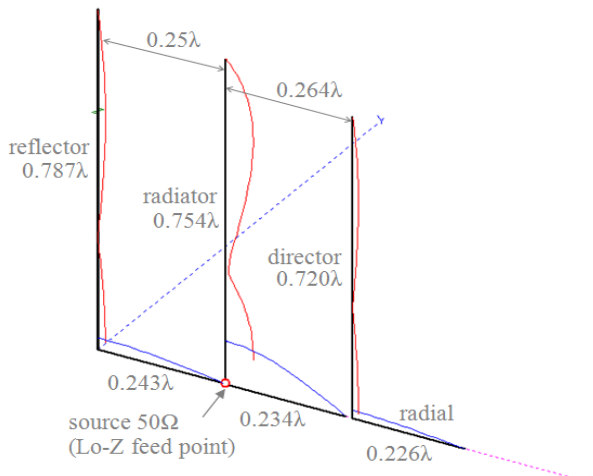


Fig. 7. Three elements  $3\lambda/4$  vertical polarized directive antenna with one radial, geometry and current distribution.

TABLE I. ELEMENT DIMENSIONS OF THE THREE QUARTER WAVELENGTH VERTICAL POLARIZED DIRECTIVE ANTENNA WITH TWO RADIALS

Element	Relative length [ $\lambda$ ]	Physical length [m]
Reflector	0.787	4.7
Reflector radial	0.243	1.45
Radiator	0.754	4.5
Radiator radial	0.234	1.395
Director	0.720	4.301
Director radial	0.226	1.35
Reflector - Radiator	0.25	1.5
Radiator - Director	0.264	1.575

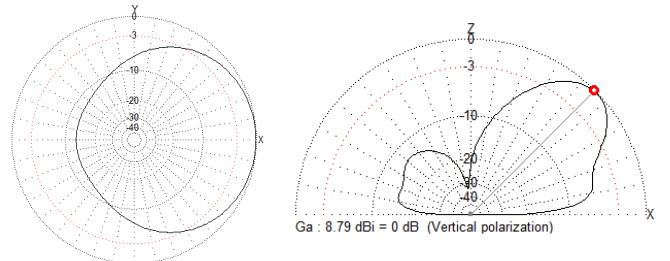


Fig. 8. Three elements  $3\lambda/4$  vertical polarized directive antenna with one radial: radiation pattern in the horizontal and vertical planes.

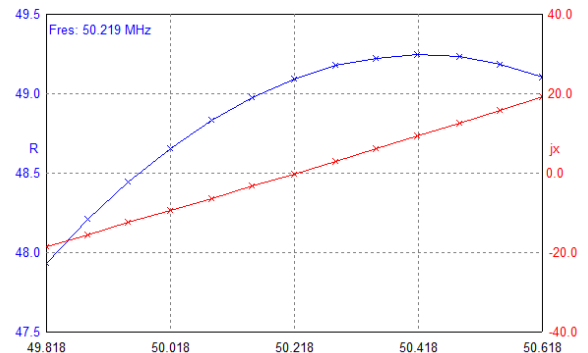


Fig. 9. Three elements  $3\lambda/4$  vertical polarized directive antenna with one radial: characteristics of the resistive (R) and reactive (X) components of the impedance.

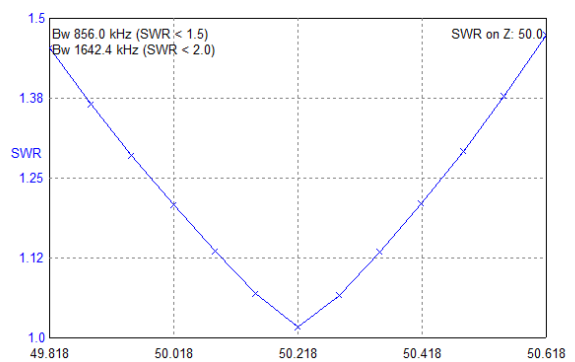


Fig. 10. Three elements  $3\lambda/4$  vertical polarized directive antenna with one radial: standing wave ratio (SWR).

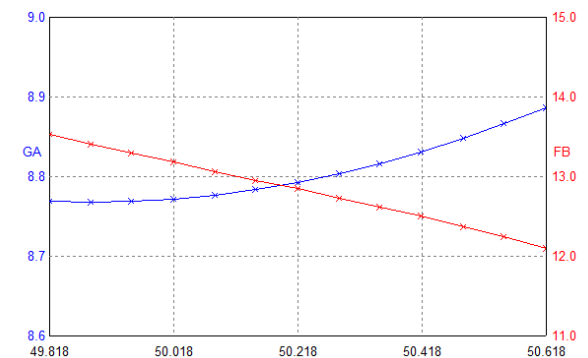


Fig. 11. Three elements  $3\lambda/4$  vertical polarized directive antenna with one radial: theoretical gain (GA) and front to back ratio (F/B).

TABLE II. PARAMETERS OF THE THREE QUARTER WAVELENGTH VERTICAL POLARIZED DIRECTIVE ANTENNA WITH ONE RADIAL

Main lobe elevation angle [ $^{\circ}$ ]	HPBW [ $^{\circ}$ ]		Ga [dBi]	F/B [dB]	Z  [ $\Omega$ ]	SWR	BW@SWR 1:1.5 [MHz]
	H	V					
43.7	124	34	8.8	12.85	49.1	1:1.02	0.856

This first design in which radial elements coplanar with the vertical elements are employed has some limitations as the distances between the vertical elements are restricted to at least  $\sim\lambda/4$  by the length of the adjacent radials. This can be overcome by the use of a quarter wavelength ( $3\lambda/4$ ) vertical radiator fitted with two radials. The parasitic elements, director and reflector, inverted T-shaped, are composed by the same one vertical element about  $3\lambda/4$  in length and two quarter wavelength horizontal elements (radials). The radials are disposed orthogonal to the plane of the vertical elements. Thus, the optimization process is more flexible, the distances between the elements become freely modifiable, following the optimization criterion used – gain, front to back ratio, half power beam width. The simulation results for this design are illustrated in Fig. 12 – 16 and are summarized in Table IV. Fig. 13 illustrates the radiation pattern in the vertical and the horizontal planes for the  $3\lambda/4$  directive antenna with two radials. In this case, the maximum gain of the antenna is 8.4 dBi at  $43^{\circ}$  elevation. Fig. 14 and 15 illustrate the simulated electrical parameters for this second antenna design. Again, at resonance, the reactive component of the impedance is close to zero and the total impedance of the antenna is about  $50\Omega$  (Fig. 14). The SWR is 1:1 and the bandwidth for an SWR < 1.5 is close to 1000 kHz (Fig. 15).

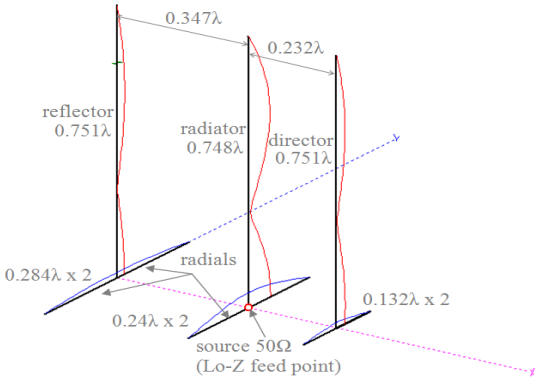


Fig. 12. Three elements  $3\lambda/4$  vertical polarized directive antenna with two radials, geometry and current distribution.

TABLE III. ELEMENT DIMENSIONS OF THE THREE QUARTER WAVELENGTH VERTICAL POLARIZED DIRECTIVE ANTENNA WITH TWO RADIALS

Element	Relative length [ $\lambda$ ]	Physical length [m]
Reflector	0.751	4.52
Reflector radials	0.284	1.708
Radiator	0.748	4.5
Radiator radials	0.240	1.442
Director	0.751	4.52
Director radials	0.132	0.792
Reflector - Radiator	0.347	2.09
Radiator - Director	0.232	1.395

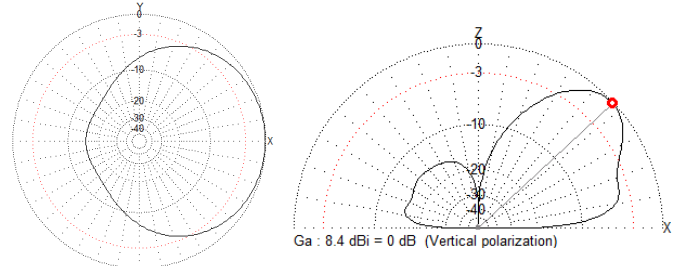


Fig. 13. Three elements  $3\lambda/4$  vertical polarized directive antenna with two radials: radiation pattern in the horizontal and vertical planes.

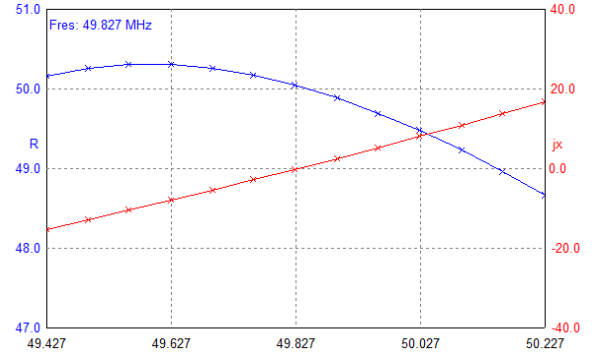


Fig. 14. Three elements  $3\lambda/4$  vertical polarized directive antenna with two radials: characteristics of the resistive (R) and reactive (X) components of the impedance.

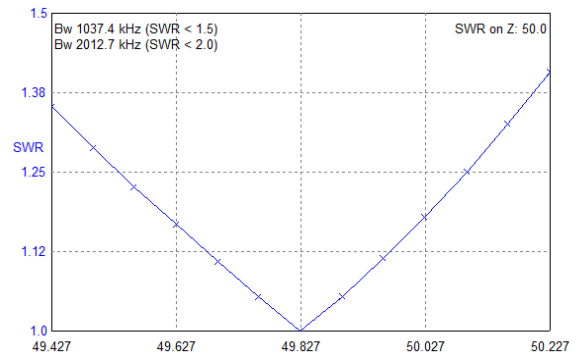


Fig. 15. Three elements  $3\lambda/4$  vertical polarized directive antenna with two radials: standing wave ratio (SWR).

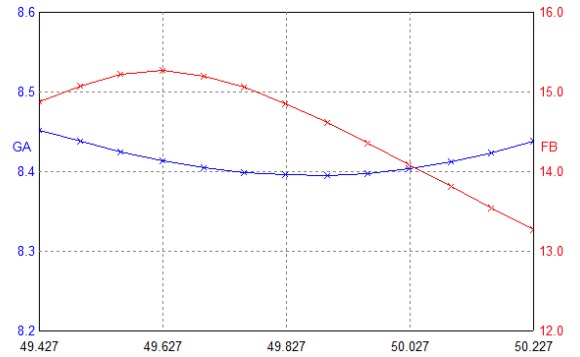


Fig. 16. Three elements  $3\lambda/4$  vertical polarized directive antenna with two radials: theoretical gain (GA) and front to back ratio (F/B).

TABLE IV. PARAMETERS OF THE THREE QUARTER WAVELENGTH VERTICAL POLARIZED DIRECTIVE ANTENNA WITH TWO RADIALS

Main lobe elevation angle [°]	HPBW [°]		Ga [dBi]	F/B [dB]	Z  Ω	SWR	BW@SWR 1:1.5 [MHz]
	H	V					
43.1	126	35	8.4	14.86	50	1:1	1.0

The three quarter wavelength vertical polarized directive antenna with three elements has a comparable radiation pattern as a three element horizontal polarized Yagi-Uda antenna. The compared total far field radiation patterns in the horizontal and the vertical planes of a three quarter wavelength vertical polarized directive antenna installed near the ground and of a horizontal polarized Yagi-Uda antenna with the radiator at a quarter wavelength AGL and the boom tilted at 30° above the horizon are shown in Fig. 17. In the horizontal plane, the radiation patterns are nearly identical, whereas in the vertical plane the Yagi-Uda antenna behaves better at high elevation angles. The disadvantage of using vertical polarization over horizontal resides in the fact of being more susceptible to artificial local interferences which are mostly vertical polarized.

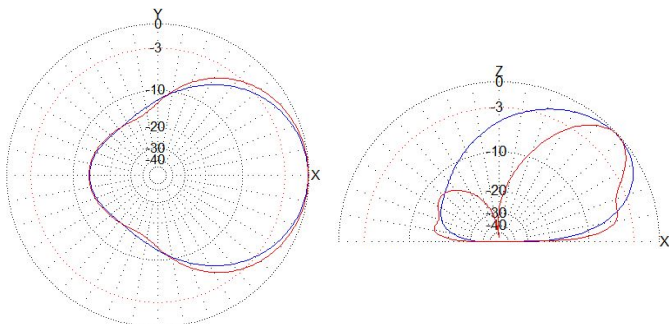


Fig. 17. Compared far field radiation patterns in the horizontal and vertical planes: three elements  $3\lambda/4$  vertical polarized directive antenna (red), three elements horizontal polarized Yagi-Uda antenna (blue).

## V. CONCLUSIONS

Based on the three quarter wavelength vertical antenna study, a new type of a directive vertical polarized antenna with the main lobe at medium elevation angles was proposed. Two designs, using one respectively two radial elements, were simulated and optimized. This type of antenna is base fed, it has low characteristic impedance and it has a low wind load. Thus, they are easy to build, allowing light structures to be used as antenna poles. For impedance matching, they do not require additional components and can be directly fed with common coaxial transmission lines, through a common mode choke. The optimizations were carried out for  $50\ \Omega$  impedance, but by tilting the radial elements they can be easily matched to a  $75\ \Omega$  impedance.

## REFERENCES

- [1] Proceedings of the Radio Meteor School 2005, International Meteor Organisation, Meteoroids: The Smallest Solar System Bodies, Proceedings of the Meteoroids Conference held in Breckenridge, Colorado, USA, May 24–28, 2010.
- [2] A. E. Rubin and J. N. Grossman, "Meteorite and meteoroid: New comprehensive definitions", Meteoritics & Planetary Science, 45: 114-122, 30 March 2010. doi:[10.1111/j.1945-5100.2009.01009.x](https://doi.org/10.1111/j.1945-5100.2009.01009.x)
- [3] Introduction to Forward Scattering Radio Techniques, International Meteor Organisation: <https://www.imo.net/observations/methods/radio-observation/intro/>
- [4] H. Griffiths, "Early history of bistatic radar," 2016 European Radar Conference (EurRAD), London, 2016, pp. 253-257.
- [5] \*\*\*, BRAMS (Belgian RAdio Meteor Stations) - <http://brams.aeronomie.be/>
- [6] H. Lamy, S. Ranvier, J. De Keyser, E. Gamby and S. Calders, "BRAMS: The Belgian RAdio Meteor Stations," 2011 XXXth URSI General Assembly and Scientific Symposium, Istanbul, 2011, pp. 1-1. doi: 10.1109/URSIGASS.2011.6050925
- [7] S. Ranvier, H. Lamy, M. Anciaux, S. Calders, E. Gamby and J. De Keyser, "Instrumentation of the Belgian RAdio Meteor Stations (BRAMS)," 2015 International Conference on Electromagnetics in Advanced Applications (ICEAA), Turin, 2015, pp. 1345-1348. doi: 10.1109/ICEAA.2015.7297336
- [8] \*\*\*, The International Project of Radio Meteor Observation - <http://www.amro-net.jp/about-hro/index-eng.html>.
- [9] W. Madkour, M.-y. Yamamoto, Y. Kakinami, S. Mizumoto, "A low cost meteor observation system using radio forward scattering and the interferometry technique," Experimental Astronomy, 2016, Volume 41, Number 1-2, Page 243
- [10] B. Bruninga, "An Omni Receive Antenna Challenge for Outernet L-band downlink reception", <http://aprs.org/outnet-whip-ant.html>.
- [11] B. Bruninga, "Antennas for APRS Satellite Igates", <http://www.aprs.org/aprs-satellite-igate-antennas.html>.
- [12] C. E. Lesanu, "ROAN Remote Radio Meteor Detection Sensor". Proceedings of the International Meteor Conference, Egmond, the Netherlands, 2-5 June 2016, Eds.: Roggemans, A.; Roggemans, P., ISBN 978-2-87355-030-1, pp. 155-158.
- [13] C. E. Lesanu and A. Done, "Parasitic circular polarized vertical antennas," 2016 International Conference on Development and Application Systems (DAS), Suceava, 2016, pp. 143-149. doi: 10.1109/DAAS.2016.7492564.
- [14] M. Mori, MMANA-GAL antenna analyzer software, <http://hamsoft.ca>
- [15] \*\*\*, NOAA Satellite and Information Service: <https://www.nesdis.noaa.gov/content/our-satellites>.
- [16] D. F. McGinnis and F. J. Eng, "NOAA remote sensing missions and frequency issues," IEEE International Geoscience and Remote Sensing Symposium. Taking the Pulse of the Planet: The Role of Remote Sensing in Managing the Environment, 2000, pp. 2452-2454 vol.6. doi: 10.1109/IGARSS.2000.859605
- [17] C. Velasco and C. Tipantuña, "Meteorological picture reception system using software defined radio (SDR)," 2017 IEEE Second Ecuador Technical Chapters Meeting (ETCM), Salinas, 2017, pp. 1-6. doi: 10.1109/ETCM.2017.8247551
- [18] C. Patil, T. Chavan and M. Chaudhari, "Hardware and software implementation of weather satellite imaging earth station," 2016 International Conference on Advances in Computing, Communications and Informatics (ICACCI), Jaipur, 2016, pp. 664-670. doi: 10.1109/ICACCI.2016.7732122
- [19] \*\*\*, NASA Goddard Space Flight Center, „NOAA-N Prime Booklet,” [https://www.nasa.gov/pdf/298662main\\_NOAA-N%20Prime%20Booklet%2012-16-08.pdf](https://www.nasa.gov/pdf/298662main_NOAA-N%20Prime%20Booklet%2012-16-08.pdf).
- [20] Tast P., [POES-APT Decoder](#), 2015.